BEM: Opening the New Frontiers in the Industrial Products Design

Zoran Andjelić

ABB Corporate Research
zoran.andjelic@ch.abb.com

Summary. Thanks to the advances in numerical analysis achieved in the last several years, BEM became a powerful numerical technique for the industrial products design. Until recent time this technique has been recognized in a praxis as a technique offering from one side some excellent features (2D instead of 3D discretization, treatment of the open-boundary problems, etc.), but from the other side having some serious practical limitations, mostly related to the full-populated, often ill-conditioned matrices. The new, emerging numerical techniques like MBIT (Multipole-Based Integral Technique), ACA (Adaptive Cross-Approximations), DDT (Domain-Decomposition Technique) seems to bridge some of these known bottlenecks, promoting those the BEM in a high-level tool for even daily-design process of 3D real-world problems.

The aim of this contribution is to illustrate the application of BEM in the design process of the complex industrial products like power transformers or switchgears. We shall discuss some numerical aspects of both single-physics problems appearing in the Dielectric Design (Electrostatics) and multi-physics problems characteristic for Thermal Design (coupling of Electromagnetic - Heat transfer) and Electro-Mechanical Design (coupling of Electromagnetic - Structural mechanics).

Nomenclature

- x - source point
- y - integration point
- $\Gamma := \partial\Omega$ - surface around the body
- σ^e - electric surface charge density $[As/m^2]$
- ρ^e - electric volume charge density $[As/m^3]$
- σ^m - magnetic surface charge density $[Vs/m^2]$
- ρ^m - magnetic volume charge density $[Vs/m^3]$
- q - charge $[As]$
- ε - dielectric constant (permittivity, absolute) $[F/m = As/Vm]$
- ε_0 - dielectric constant of free space (permittivity)$=1/\mu_0 c_0^2 \approx 0.885419e^{-11}$
- c_0 - speed of electromagnetic waves (light) in vacuum$= 2.2997925e^8$ $[m/s]$
- ε_r - relative dielectric constant

- μ - magnetic permeability (absolute) $[H/m]$
- μ_0 - magnetic permeability of the free space $[H/m] = 4\pi/10^7$
- μ_r - relative magnetic permeability
- σ - electrical conductivity $[Sm/mm^2]$
- $\boldsymbol{E}$ - electrical field strength $[V/m]$
- $\boldsymbol{D}$ - electrical flux (displacement) density $[As/m^2]$
- φ - electrical potential $[V]$
- I - electrical current $[A]$
- U - electrical voltage $[V]$
- $\varphi^{ext}(I)$ - potential of the external electrostatic field [V]
- $\mathbf{H}$ - magnetic field strength $[A/m]$
- $\mathbf{B}$ - magnetic flux density $[T]$
- $\boldsymbol{F}$ - force $[N]$
- $\mathbf{f}_v$ - volume force density $[N/m^3]$
- $\mathbf{f}_m$ - magnetic force density $[N/m^3]$
- $\mathbf{f}_m^s$ - "strain" magnetic force density $[N/m^3]$
- $\mathbf{J}$ - current density $[A/m^2]$
- $\mathbf{J}_0$ - exciting current density $[A/m^2]$
- $\mathbf{S}$ - Poynting vector
- $\bar{f}$ - time-average force density $[N/m^3]$ (volume) or $[N/m^2]$ (surface)
- Θ - solid angle
- $\mathbf{j}$ - current density (complex vector) $[A/m^2]$
- ω - angular velocity $[rad/s]$
- f - frequency $[Hz]$
- T - temperature $[^oC]$ or $[K]$
- α - heat transfer coefficient $[W/m^2K]$

1 Introduction

One of key challenges in a booming industrial market is to achieve a better *time2market* performance. This marketing syntagma one could translate as: "To be better (best) in a competition race, bring the product to the market in the fastest way (read cheapest way), simultaneously preserving / improving its functionality and reliability". One of the nowadays unavoidable ways to achieve this target is to replace partially (or completely) the traditional *Experimentally-Based Design* (EBD) with the *Simulation-Based Design* (SBD) of industrial products. Usage of SBD contributes in:

- Acceleration of the design process (avoiding prototyping),
- Better design through better understanding of the physical phenomena,
- Recognizability of the product's weak points already at the design stage.

Introduction of the SBD in the design process requires accurate, robust and fast numerical technologies for:

- **3D real-world problems** analysis, preserving the necessary structural and physical complexity,
- ... but using the numerical technologies enough **user-friendly** to be accepted by the designers,
- ... and using the numerical technologies suitable for the **daily design** process.

All these three items present quite tough requirements when speaking about the industrial products that are usually featured by huge dimensions, huge aspect ratio in model dimensions, complex physics, complex materials. For the class of the problems we are discussing here, there are basically two candidates among many numerical methods that could potentially be used: FEM (Finite Element Method) and BEM (Boundary Element Method). Our experience shows that for the electromagnetic and electromagnetically-coupled problems BEM has certain advantages when dealing with complex engineering design.

Without going into details, let us list some of the main BEM characteristics:

- Probably the most important feature of BEM is that for *linear* classes of problems the discretization needs to be performed only over the interfaces between different media. This excellent characteristic of BEM makes the discretisation/meshing of complex 3D problems more straightforward and usable for simulations in a *daily design* process.
- Also, this feature is of utmost importance when dealing with the simulation of *moving boundary problems*. Thanks to the fact that the space between the moving objects does not need to be meshed, BEM offers an excellent platform for the simulation of *dynamics*, especially in 3D geometry.
- Furthermore, the *open boundary problem* is treated easily with BEM, without need to take into account any additionally boundary condition. When using tools based on the differential approach (FEM, FDM), the *open boundary problem* requires an additional *bounding box* around the object of interest, which has a negative impact on both mesh size and computation error.
- Another important feature of BEM is its *accuracy*. Contrary to differential methods, where *adaptive mesh refinement* is almost imperative to achieve the required accuracy, with BEM it is frequently possible to obtain good results even with a relatively rough mesh. But, at this point we also do not want to say that "adaptivity" could not make life easier even when using BEM.

In spite of the above mentioned excellent features of BEM, this method had until recent time some serious limitations with respect to the practical design, mostly related to the:

- full populated matrix,
- huge memory requirements,

- bad matrix conditioning.

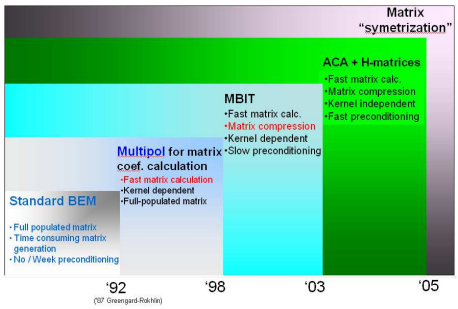

Fig. 1. Paradigm change in BEM development

Thanks to the real breakthroughs happening in the last decade in BEM-related applied mathematics, most of these bottlenecks have been removed. To author's opinion the work done by Greengard and Rochlin, Greengard [10], is probably one of the crucial ignitions contributing to this paradigm change, Figure 1. Today we can say that this work, together with a number of capital contributions of other groups working with BEM, has lunched really a new dimension in the simulation of the complex real-world problems. In the following we shall try to illustrate it on some practical examples like:

- Dielectric design of circuit breakers,
- Electro-mechanical design of circuit breakers,
- Thermal design for power transformers.

2 Dielectric Design of Circuit Breakers

Under **Dielectric Design** we usually understand the *Simulation-Based Design* (SBD) of configurations consisting of one or more electrodes loaded with either *fixed* or *floating* potential and being in contact with one or more dielectric media. From the physics point of view, here we deal with a *single-physics* problem, which can be described either by a Laplace or Poisson equation.

2.1 Briefly About Formulation

For 3D BEM analysis of electrostatic problems, the equations satisfying the field due to stationary charge distribution can be derived directly form the Maxwell equations, assuming that all time derivatives are equal to zero. The formulation can be reduced to the usage of I and II Fredholm integral equations[1]:

[1] The complete formulation derivation can be found in Tozoni [19], Koleciskij [15]

$$\varphi(x) = \varphi^{ext}(x) + \frac{1}{4\pi\varepsilon_0} \sum_{m=1}^{M} \int_{\Gamma_m} \sigma^e(y) K_1 d\Gamma_m(y) \tag{1}$$

$$\sigma^e(x) = \frac{\lambda}{2\pi} \sum_{m=1}^{M} \int_{\Gamma_m} \sigma^e(y) \frac{\mathbf{r} \cdot \mathbf{n}}{r^3} d\Gamma_m(y) \tag{2}$$

where $\varepsilon = \varepsilon_0 \cdot \varepsilon_r$ is absolute permittivity with $\varepsilon_0 = 8.85 \cdot 10^{-12} F/m$ the permittivity of the free space and ε_r the relative permittivity or dielectric constant, $K_1 = \frac{1}{r} = \frac{1}{|\mathbf{x}-\mathbf{y}|}$ is a *weakly singular* kernel, r is a distance between the calculation point x and integration point y, $\mathbf{n}$ is a unit normal vector in point x directed into the surrounding medium, and $\lambda = \frac{\varepsilon_i - \varepsilon_e}{\varepsilon_i + \varepsilon_e}$.
The equation (1) is usually applied for the points laying on the electrodes, and the equation (2) is applied for the points positioned on the interface between different dielectrics. Then the electrostatic field strength at any point in the space can be determined as:

$$\mathbf{E}(x) = -\nabla\varphi(x) = -\frac{1}{4\pi\varepsilon_0} \sum_{m=1}^{M} \int_{\Gamma_m} \sigma^e(y) \cdot \nabla K_1 d\Gamma_m(y) \tag{3}$$

whereby the position vector $\mathbf{r} = \mathbf{x} - \mathbf{y}$ in K_1 is pointed towards the collocation point x. The discretization of equations (1) and (2) yields a densely populated matrix, which is well known as the major bottleneck in BEM computations. The amount of storage is of order $O(N^2)$, with N being the number of unknowns. Furthermore, the essential step at the heart of the iterative solution of this system is a matrix-vector multiplication and the cost of such a multiplication is also of order $O(N^2)$. Thus a reduction of the complexity to $O(N \log N)$ or $O(N)$ would naturally be very desirable. Developments started with a seminal paper by Greengard [10] that proposed a *Fast Multipole Method*, which became highly popular in several numerical communities. Another fundamental development was brought about by Hackbusch [11, 12]. In the following we present a brief description of MBIT[2] algorithm that is used in our computations. The central idea is to split the discretized boundary integral operator into a *far-field* and a *near-field* zone. The singularity of the kernel of the integral operator is then located in the *near-field*, whereas the kernel is continuous and smooth in the *far-field*. Compression can then be achieved by a separation of variables in the *far-field*. In order to reach this goal, the boundary in the first stage is subdivided into clusters of adjacent panels that are stored in a hierarchical structure called the panel-cluster tree. The first cluster is constructed from all elements/panels (the largest set of elements/panes) and is denoted as x_{00}, Figure 2. We continue to subdivide each existing cluster level successively into smaller clusters with cluster centers x_{ij} through bifurcation, Figure 2a. After several bifurcations we obtain

[2] Multipole-Based Integral Technique

a cluster tree structure for the elements/panel set, Figure 2b. Then, in the

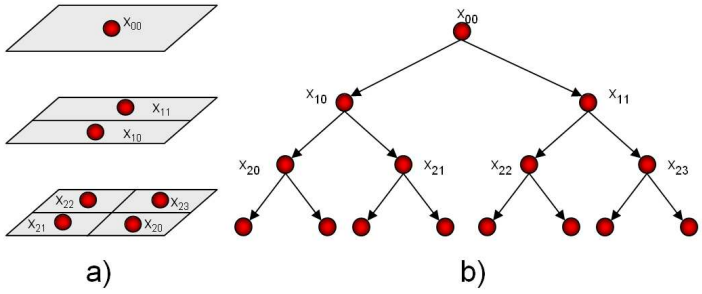

Fig. 2. a)Panel bifurcation, b)Panel cluster tree

second stage we collect all admissible pairs of clusters, i.e. pairs that fulfill the admissibility condition $|\mathbf{x}-\mathbf{x}_0|+|\mathbf{x}^c-\mathbf{x}_0^c| \leq \eta\,|\mathbf{x}_0-\mathbf{x}_0^c|$ where $0 \leq \eta < 1$ into the far-field block. The centers of gravity of the panel clusters and node/vertex clusters are here denoted by $\mathbf{x}_0$, $\mathbf{x}_0^c$, respectively. All other pairs of clusters (the non-admissible ones) belong to the *near-field*. Then the matrix entries corresponding to the *near-field* zone are computed as usual, whereas the matrix blocks of the *far-field* are only approximated. This is achieved by an expansion of the kernel function $k(\mathbf{x},\mathbf{x}^c)$ that occurs in the matrix entries

$$a_{ij} = \int_\Gamma \int_\Gamma \hat{\varphi}_i(\mathbf{x}) k(\mathbf{x},\mathbf{x}^c) \varphi_j(\mathbf{x}^c) d\Gamma(x) d\Gamma(x^c)\,. \tag{4}$$

The expansion:

$$k(\mathbf{x},\mathbf{x}^c) \approx k_m(\mathbf{x},\mathbf{x}^c;\mathbf{x}_0,\mathbf{x}_0^c) = \sum_{(\mu,\nu)\in \mathrm{I}_m} k_{(\mu,\nu)}(\mathbf{x},\mathbf{x}_0^c) X_\mu(\mathbf{x},\mathbf{x}_0) Y_\nu(\mathbf{x}^c,\mathbf{x}_0^c) \tag{5}$$

decouples the variables $\mathbf{x}$ and $\mathbf{x}^c$ and must be done only in the *far-field*. Then, the matrix-vector products can be evaluated as:

$$\nu = \tilde{A}\cdot u = N\cdot u + \sum_{(\sigma,\tau)\in F} X_\sigma^T (F_{\sigma,\tau}(Y_\tau \cdot u))\,. \tag{6}$$

Several expansions can be used for this purpose: Multipole-, Taylor- and Chebyshev-expansion. The procedures lead to a low rank approximation of the *far-field* part and it is shown in Schmidlin [17] that one obtains exponential convergence for a proper choice of parameters. A more detailed elaboration and comparison of all three type of expansions can also be found in the same reference.

Example 1: **SBD *for a Generator Circuit-Breaker Design***

In this example it is briefly shown how Simulation-Based Design of the Generator Circuit-Breaker (GCB) is performed using a BEM[3] module for electrostatic field computation.

Generator circuit-breakers, Figure 3, are important components of electricity transmission systems. Figure 4 (left) shows the complete assembly of a GCB containing, beside the interrupting chamber as a key component, all other parts such as current and voltage transformers, earthing switches, surge capacitors, etc. The simulation details for the above shown generator circuit-breakers case were:

Fig. 3. ABB generator circuit-breaker

- The discretization of the model has been performed using *second order* triangle elements.
- The stiffness matrix has been assembled using an *Indirect* Ansatz with *collocation* in the main triangle vertices, formulas (1) and (2). It has to be mentioned here that in both the real design and consequently then in the simulation model, geometrical singularities like edges and corners have been removed through *rounding*. In the real design this is a common practice in all high-voltage devices in order to prevent the occurrence of *dielectric breakdown*. On the numerics side, this fact enables usage of the *nodal collocation* method - which is also the fastest one - without violating the mathematical correctness of the problem.
- The coefficients of the stiffness matrix have been calculated using the **multipole approach**, Greengard [10], with *monopole*, *dipole* and *quadropole* approximations for the far-field treatment, Andjelic [3]. *Diagonal matrix preconditioning* has been used, which enables fast and reliable matrix solution using GMRES. This run has been accomplished without any matrix compression, but using a parallelized version of the code, Blaszczyk [7]. For a parallel run we used a PC cluster with 22 nodes. The data about memory and CPU time are given in Table 1.
- The calculated electrostatic field distribution is shown in Figure 4 (right). It can be seen that the highest field strength appears on the small feature details, such as screws.

Validation:

Replacement of the EBD with the SBD requires a number of field tests to confirm the simulation results by the experiments. Validation is one of important

[3] This BEM module is a sub-module for electrostatic analysis in POLOPT (http://www.poloptsoftware.com), a 3D BEM-based simulation package for single and multi-physics computation.

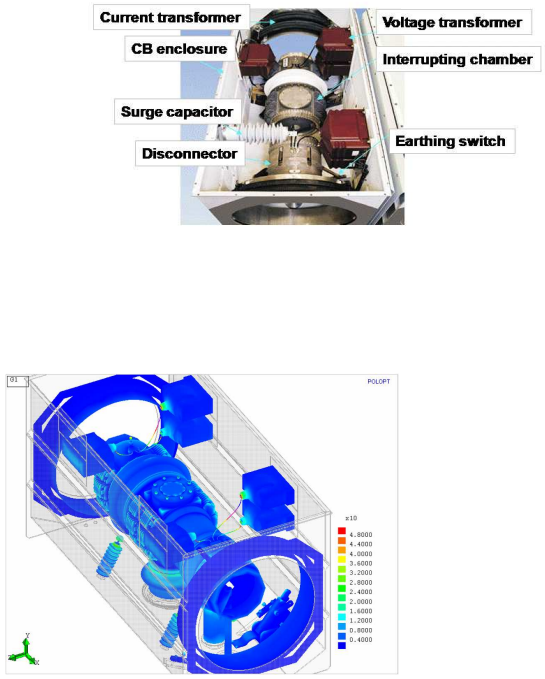

Fig. 4. GCB assembly (left). ABB Generator Circuit-Breaker: Electrostatic field distribution, E[V/m] (right)

Table 1. The analysis data for GCB example.

Elements	*Nodes*	*Main vertices*	*Memory*	*CPU*
145782	291584	80230	42GByte	2h20’

steps to gain the confidence in the simulation tools. Figure 5 (right) shows the experimental verification of the results obtained by the simulation of the GCB.

Note 1:
Calculated field distribution is just a “primary” information for the designers. For complete judgment about the products behavior, it is usually necessary to go one step forward, i.e. to evaluate the *design criteria*. Very often such criteria are based on the analysis of the field lines, Figure 5 (left), that enables further the conclusion about the breakdown probability in the inspected devices.

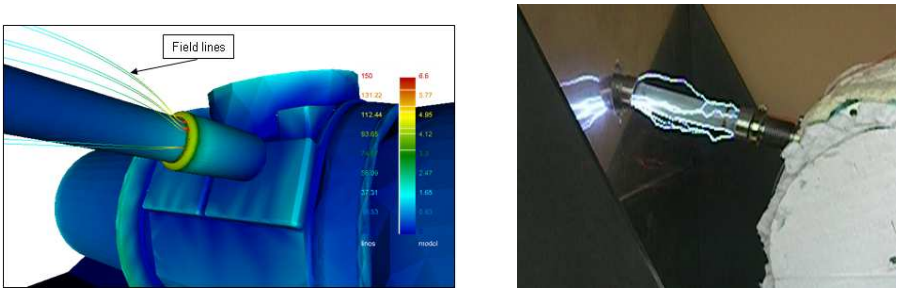

Fig. 5. Electric field strength distribution - detailed view including field lines traced from the position of the maximal field values (left). Experimental verification of the simulation results (right)

3 Electro-Mechanical Design of Circuit Breakers

In Electro-Mechanical class of problems we are dealing with coupled electromagnetic / structural-dynamic phenomena. Better to say, we are seeking to find out what is a mechanical response of the structure subjected to the action of the electromagnetic forces. Coupling of these phenomena can be either *weak* or *strong*. Under *weak* coupling we understand the sequential analysis of each phenomena separately, coupled together via an iterative scheme. In *strong* coupling we usually deal with the simultaneous solution of both problems, whereby the coupling is preserved on the equations level. In the present material we deal with the *weak* coupling, that usually assumes two main steps:

- Calculation of electromagnetic forces
- Calculation of mechanical response

Forces evaluation is a first step in this coupled simulation chain. Electromagnetic forces appear in any device conducted by either DC or AC current, or subjected to the action of an external electromagnetic field[4,5]. Force analysis itself is a bright field and will not be treated in details within this material. More info can be found in Andjelic [4]. Here we shall give only a brief overview on the Workflow for coupled EM-ME simulation tasks, Figure 6. A very first

[4] In this material we shall not treat the electro-mechanical problems whereby the force are of electrostatic origin.

[5] In certain applications (force sensors, pressure sensors, accelerometers) we are not looking for *mechanical response* caused by the electromagnetic forces, but rather for *electrical response* caused by the mechanical forces (*piezoelectric problem*). This case will not be covered in the scope of this material. More information about BEM treatment of these classes of problems can be found in Gaul [9], Hill [14]. Here we shall also not cover the topic of coupled Electro-Magnetic / Mechanics problems related to magnetostriction phenomena (change of the shape of magnetostrictive material under the influence of a magnetic field). More information for example in Whiteman [20].

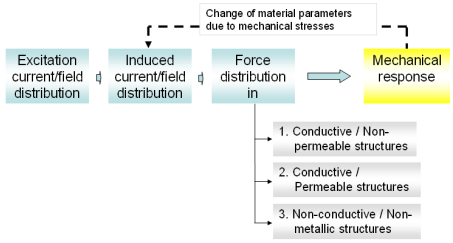

Fig. 6. Weak coupling scheme for EM-SM problems

step in the simulation chain is the calculation of the excitation current / field distribution. The calculation of the stationary current distribution in the conductors assumes the solution of the Laplace problem, analogous to the previously described electrostatic case. A detailed description of the formulations for stationary current calculation can be found in Andjelic [4]. When performing a coupled electromagnetic-structural mechanics analysis, we are not interested in the *total force*, but rather in the *local force* density distribution. For stationary case the local force density (**forces per unit volume**, $[N/m^3]$) can be calculated as:

$$\mathbf{f}_m = \mathbf{J} \times \mathbf{B} - \frac{1}{2} H^2 \nabla \mu + \mathbf{f}_m^s \,. \tag{7}$$

Usually in praxis we are interested in the time-averaged force density $\bar{f}$ $[N/m^3]$:

$$\bar{f} = \frac{1}{2} \mathrm{Re} \left\{ \rho^e \mathbf{E}^* + \mathbf{J} \times \mathbf{B}^* + \rho^m \mathbf{H}^* + \mathbf{M} \times \mathbf{D}^* \right\} \tag{8}$$

where $\mathbf{M} = i\omega \mathbf{P}^m = i\omega\mu_0(\mu_r - 1)\mathbf{H}$ are the bounded magnetic currents, and ρ^m are the bounded magnetic charges.
Basically, we can distinguish between the forces acting on:

- conductive/non-permeable structures,
- conductive/permeable structures[6],
- non-conductive/non-permeable structures[7].

If we stay with the typical design cases appearing in the transformers and circuit-breakers design, that the mostly encountered problems are related to the forces in conductive/non-permeable structures (bus-bars, windings). For time-average Lorentz force density in a non-permeable current-carrying conductor (μ=1), the equation (7) reduces to:

$$\bar{f} = \frac{1}{2} \mathrm{Re} \left\{ \mathbf{J} \times \mathbf{B}^* \right\} \,. \tag{9}$$

[6] More on the force analysis on conductive/permeable structures can be found in Henrotte [13].

[7] This class of problems is rather seldom and appears mostly in sensor design, Andjelic [1].

These local forces are then further passed as an *external load* for the analysis of the mechanical quantities, last module in Figure 6. BEM formulations used in our module for linear elasticity problems is described in more details in Andjelic [4].

Example 2: ***Electro-mechanical Design of Generator Circuit-Breaker***

Let us consider now the coupled electromechanical loading of a switch found in the generator circuit breaker (GCB) seen already in the previous example. Following a current-distribution and eddy-current analysis, it is possible by Biot-Savart calculation to find the body-forces arising out of Lorentz interactions. In fact, these forces are often of interest only in a limited region of the entire engineering system, typically in moving parts. In the GCB case presented here, a point of particular interest is the "knife" switch, where there is a tendency for the generated Lorentz forces to act so as to open the switch. Taking the example from earlier, for the mechanical part of the analysis only a limited portion of the mesh needs to be evaluated. Results were calculated using a mesh comprising 4130 triangular planar surface elements and 2063 nodes. The volume discretization (necessary for the body-force coupling) com-

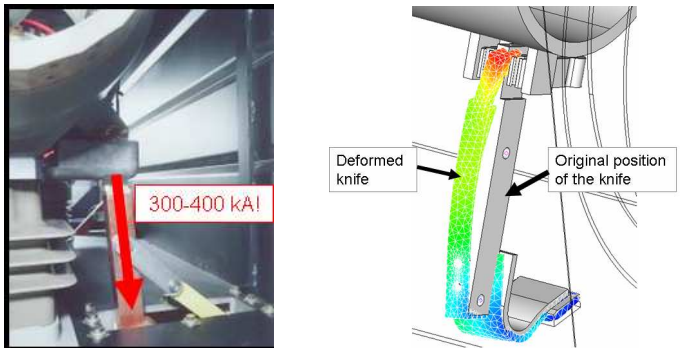

Fig. 7. A detail of the earthing-switch in GCB carrying the current of 300-400 kA! (left). Deformation of the earthing knife (overscaled), caused by the action of the short-circuit forces (right).

.

prises 14000 tetrahedra. This model has been analyzed taking advantage of the ACA approximation for the single and double layer potentials described earlier in the outline of the formulation. Results from this analysis are shown in Figure 7 (right). Clearly visible is the effect of the coupling forces on the switch, which has a tendency to move out of its closed position under the action of the electromagnetic loading. This quantitative and qualitative information is a valuable input into the design process leading to the development of complex electromechanical systems.

4 Thermal Design for Power Transformers

When speaking about the Thermal Design we are usually looking for thermal response of the structures caused by the electromagnetic losses. In reality, the physics describing this problem is rather complex. There are three major physical phenomena that should be taken into account simultaneously: the electromagnetic part responsible for the losses generation, a fluid part responsible for the cooling effects and thermal part responsible for the heat transfer. Simulation of such problems, taking into account both complex physics and complex 3D structures found in the real-world apparatus is still a challenge, especially with respect to the requirements mentioned at the beginning: *accuracy-robustness-speed*. A common practice to avoid a complex analysis of the cooling effects by a fluid-dynamics simulation is to introduce the *Heat-Transfer Coefficients* (HTC) obtained either by simple analytical formulae, (see for example Boehme [8]) or based on experimental observations. For this type of analysis the link between the electromagnetic solver and heat-transfer solver is throughout the *losses* calculated on the electromagnetic side and passed further as *external loads* to the heat-transfer module.

4.1 Workflow

The Workflow used for the coupled simulation of electro-magnetic / thermal problems is shown in Figure 8. Usually the very first step in thermal simula-

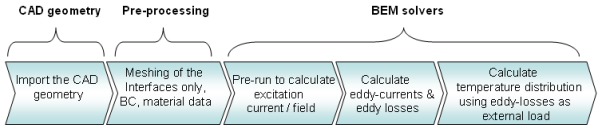

Fig. 8. EM-TH Workflow

tion the industrial products like power transformer is import of the geometry from CAD tool, followed by meshing and setting appropriate boundary conditions (BC) and material data. It has to be stressed again that thanks to the excellent features of BEM, we can solve such complex diffusion problem by meshing only the interfaces between different media, i.e. avoiding completely any volume mesh[8]! The solution phase consist of three major steps: calculation of the excitation current distribution, calculation of the eddy-currents / losses distribution and finally calculation of the temperature distribution. Let us give a brief outline on the eddy-current formulation, as one of the probably

[8] This is valid so long we are working with linear problems. In the case when non-linear problem has to be treated, than when using BEM it is necessary to apply the volume mesh, but only for the parts having non-linear material behavior!

most complicated problems in the computational electromagnetics. More info on the formulations of excitation current as well as thermal calculation can be found in Andjelic [4].

4.2 Eddy-current Analysis

There are a number of possible formulation that can be used for BEM-based analysis of eddy-current problems. A useful overview of the available eddy-current formulations can be found in Kost [16]. Here we follow the $H-\varphi$ formulation, whereby for the treatment of the skin-effect problems an modified version of this formulation is used, Andjelic [2]. The $H-\varphi$ formulation is based on the *indirect* Ansatz, leading thus to the minimal number of 4 degrees of freedom (DoF) per node[9]. This nice feature makes this formulation suitable for the eddy-current analysis of complex, real-world problems. The $H-\varphi$ formulation need to be used with a care in cases where the problem is *multi-valued*, i.e. when the model belongs to the class *multi-connected problems*, Tozoni [19]. The following integral representation is used[10]:

$$\begin{aligned}
&\tfrac{1}{2}\mathbf{j}(x) + \tfrac{1}{4\pi}\oint_{\Gamma}\mathbf{n}(x)\times\left(\mathbf{j}(y)\times\nabla\tfrac{e^{-(1+i)k\cdot r}}{r}\right)d\Gamma(y) - \\
&\tfrac{1}{4\pi}\oint_{\Gamma}\sigma^m(y)(n(x)\times\nabla\tfrac{1}{r}d\Gamma(y) \qquad (10)\\
&= -\mathbf{n}(x)\times\mathbf{H}_0(x)\\
&\quad \tfrac{1}{2}\sigma^m(x) + \tfrac{1}{4\pi}\oint_{\Gamma}\sigma^m(y)\cdot\mathbf{n}(x)\cdot\nabla(\tfrac{1}{r})d\Gamma(y) + \\
&\quad \tfrac{\mu}{4\pi\mu_0}\oint_{\Gamma}\mathbf{n}(x)\left(\mathbf{j}(y)\times\nabla\tfrac{e^{-(1+i)k\cdot r}}{r}\right)d\Gamma(y) \qquad (11)\\
&\quad = -\mathbf{n}(x)\cdot\mathbf{H}_0(x)\,.
\end{aligned}$$

This boundary integral equation system can be written in operator form:

$$\begin{bmatrix} A_1 & B_1 \\ B_2 & A_2 \end{bmatrix}\begin{pmatrix}\mathbf{j}\\ \sigma^m\end{pmatrix} = \begin{pmatrix}-2\mathbf{n}\times\mathbf{H}_0\\ -2\mathbf{n}\cdot\mathbf{H}_0\end{pmatrix}\,. \qquad (12)$$

For more details on a numerical side of this approach the reader is referred to Schmidlin [18]. Solution of the equation system (12) gives the virtual magnetic charges σ^m and virtual current density $\mathbf{j}$. Then, the magnetic field in conductive materials can be expressed as:

$$\mathbf{H}^+(x) = \frac{1}{4\pi}\oint_{\Gamma}\nabla\times[\mathbf{j}(y)K(x,y)]\,d\Gamma(y); \qquad x\in\Omega^+; y\in\Omega^+ \qquad (13)$$

[9] With $H-\varphi$ formulation it is possible to work even with only 3 DoF/node, whereby the eddy-currents on the surfaces are described in a *surface* coordinate system instead of Cartesian, Yuan [21].

[10] For complete derivation of the above formulations, please look in Kost [16], Tozoni [19], Andjelic [2]

and

$$\mathbf{H}^{-}(x) = \mathbf{H}o(x) - \frac{1}{4\pi}\oint_{\Gamma} \sigma_m(y)\nabla_x G(x,y)d\Gamma(y) \qquad x \in \Omega^{-}; y \in \Omega^{-} \quad (14)$$

in the non-conductive materials. $\mathbf{H}_0$ is the primary magnetic field produced by the exciting current $\mathbf{J}_0$ and $K = e^{-(1+i)k\cdot\mathbf{r}}/r$, $G = 1/r$.

Fast BEM for Eddy-current Analysis

Although the above formulation is the minimal-order formulation for 3D eddy-current analysis, it still reaches very fast the limits (both in memory and CPU) when trying to apply it to the simulation of the complex real-world problems. As said at the very beginning, the new emerging techniques like MBIT or ACA have enabled the efficient usage of this (and other BEM-based formulations) by removing most of the known bottlenecks (huge memory, big CPU, bad matrix conditioning). MBIT has enabled the efficient matrix generation, together with low-memory matrix compression. For a pity, when using MBIT an extra preconditioner is necessary in the case of bad conditioned matrices (for example Schur-complement). ACA from other side covers all three major critical points. Beside fast matrix generation, excellent compression, ACA provides also inherently the matrix preconditioning, Bebendorf [6], Bebendorf [5]. As illustration, Figure 9 shows a comparison of MBIT and ACA versus dense matrix solution.

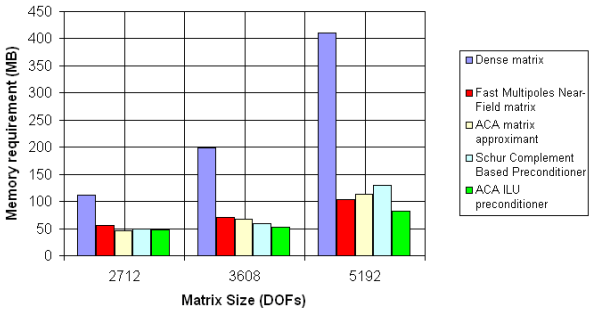

Fig. 9. Memory requirements for various matrix compression and preconditioning methods

---

Example 2: ***Thermal Design of Power Transformers***

The procedure described above has been used for the analysis of a number of power transformer problems, both single- and three-phase units, Figure 10

(left). Figure 10 (right) shows the distribution of the calculated excitation field over the transformer tank wallfootnote, together with the three-phase bus-bars structure. It has to be noted that typical transformers structures (for

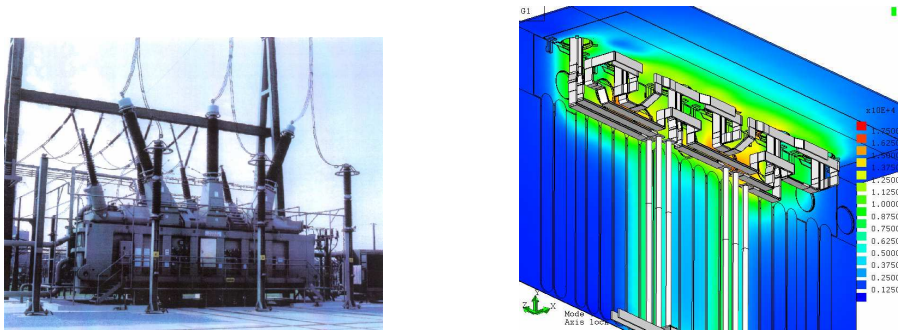

Fig. 10. 985 MVA Power Transformers, ABB (left). Excitation field distribution in the three-phase transformer bus-bars (right)

example tank or turrets) usually consist of one or more components made of different materials like magnetic or non-magnetic steel, copper or aluminum. The numerical procedure that are used have to be careful selected in order to properly resolve the penetration of electro-magnetic field into each of these materials, depending on their magnetic permeability, electrical conductivity and applied frequency. Calculation of eddy currents and losses is performed using the above described numerical procedure. Figure 11 shows the distribution of the calculated eddy-currents.

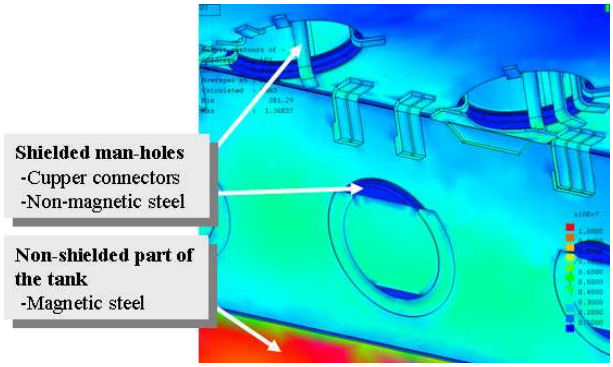

Fig. 11. Eddy current distribution (complex magnitude)- detailed view to the inner shielding details

Validation

As mentioned before, an important aspect of the practical usage of the simulation tools is its validation, i.e. its comparison with the measured data. In the following example we present as illustration the comparison between simulated and measured temperature for an 400 MVA single-phase transformer unit.[11]More on BEM-based approach for temperature analysis can be found in Andjelic [4]. The temperature calculation is obtained using previously cal-

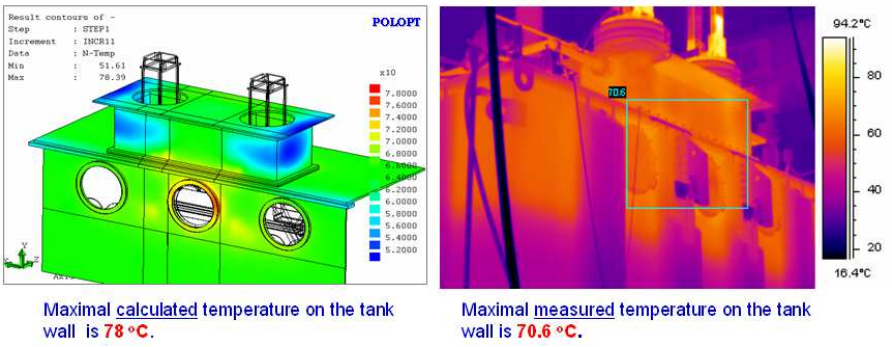

Fig. 12. Validation

culated eddy losses as the external load for thermal run. The impact of the cooling effects is taken into account by the appropriate choice of the heat transfer coefficients. The simulation output has been validated by comparison with thermography recording done during the transformer operation. Figure 12 shows the comparison between the simulation results and the measured results obtained by the thermography. It can be seen that the simulation results have good agreement with the measured results. The difference between the measured and calculated results (10% in this case) could be probably explained by the inaccurate estimation of the heat transfer coefficients used in the simulation.

5 Some Concluding Remarks

In this paper we have tried to illustrate some BEM-based approaches for the simulation of different problems appearing in engineering design praxis. The excellent features of BEM for both single and multi-physics tasks are highlighted, together with some emerging numerical techniques like MBIT and

[11] The parts of the tank exposed to the thermal overheating are often made of the non-magnetic steel. This allows usage of the linear Ansatz for eddy-current class of problems.

ACA, recognized as the major drivers leading to the real breakthrough in BEM usage for practical design tasks.
But, beside these and many other good features of BEM, and staying at the level of *static* or *quasi-static* simulation tasks, there are still a number of potential improvements that could be made to achieve the "best in the class" tool desired for the advanced simulations in the industrial design (*strong* coupling formulations, non-linearity treatment, contact problems, preconditioning etc.).
In spite of these and other open issues, the authors general opinion is that the BEM already now offers an excellent platform for successful simulation of 3D real-world industrial problems. Especially when speaking about some of the major requirements appearing in the Simulation-Based Design nowadays, like:

- *assembly* instead of *component simulation*,
- simulation for the *daily* design process,
- *user-friendly* simulation, but still preserving the *full geometrical and physical complexity*,

BEM-based numerical technologies seems to fulfill the majority of the requirements needed today for efficient design of the industrial products.

References

[1] Z. Andjelić, P. Kripner, and A. Vogel. Simulation based design of O2 MEMS sensor. *Fifth Inter. Conf. on Modeling and Simulation of Microsystems*, 2002.
[2] Z. Andjelić, B. Krstajić, S. Milojković, A. Blaszczyk, H. Steinbigler, and M. Wohlmuth. *Integral Methods for the Calculation of Electric Fields*, volume 10. Scientific Series of the Internaltional Bureu, Forschungszentrum Jülich GmbH, 1992.
[3] Z. Andjelić and P. Marchukov. Acceleration of the electrostatic computation using multipole technique. Technical report, ABB Corporate Research, Heidelberg, 1992.
[4] Z. Andjelić, J. Smajić, and M. Conry. *Boundary Integral Analysis: Mathematical Aspects and Applications*, chapter BEM-based Simulations in Engineering Design. Springer-Verlag, 2007.
[5] M. Bebendorf and S. Rjasanow. Adaptive low rank approximation of collocation matrices. *Computing*, 70:1–24, 2003.
[6] M. Bebendorf, S. Rjasanow, and E.E. Tytyshnikov. Approaximations using diagonal-plus skeleton matrices. *Chapman & Hall/CRC Research Notes in Mathematics*, 414:45–53, 1999.
[7] A. Blaszczyk, Z. Andjelić, P. Levin, and A. Ustundag. *Lecture Notes on Computer Science*, chapter Parallel Computation of Electric Fields in

a Heterogeneous Workstation Cluster, pages 606–611. Springer Verlag Berlin Heidelberg, hpcn europe 95 edition, 1995.

[8] H. Boehme. *Mittelspannungstechnik*. Verlag Technik GmbH Berlin-München, 1972.

[9] L. Gaul, M. Kögl, and M. Wagner. *Boundary Element Methods for Engineers and Scientists*. Springer-Verlag Berlin, 2003.

[10] L. Greengard and V. Rokhlin. A fast algorithm for particle simulations. *J. Comput. Phys.*, 73:325–348, 1987.

[11] W. Hackbusch. The panel clustering technique for the boundary element method. *9th Int. Conf. on BEM*, pages 463–473, 1987.

[12] W. Hackbusch and Z.P. Nowak. On the fast matrix multiplication in the boundary element method by panel clustering. *Numer. Math.*, 54:463–491, 1989.

[13] F. Henrotte and K. Hameyer. Computation of electromagnetic force densities: Maxwell stress tensor vs. virtual work principle. *J. Comput. Appl. Math.*, 168(1-2):235–243, 2004.

[14] L.R. Hill and T.N. Farris. Three-dimensional piezoelectric boundary element method. *AIAA Journal*, 36(1), January 1998.

[15] E.C. Koleciskij. Rascet eletriceskih poljei ustroistv visokog naprezenija. *Energoatomizdat*, 1983.

[16] A. Kost. *Numerische Methoden in der Berechnung Elektromagnetischer Felder*. Springer Verlag, 1994.

[17] G. Schmidlin. Fast Solution Algorithms for Integral Equations in $\mathbb{R}^3$. Master's thesis, ETH Zurich, 2003.

[18] G. Schmidlin, U. Fischer, Z. Andjelić, and C. Schwab. Preconditioning of the second-kind boundary integral equations for 3D eddy current problems. *Internat. J. Numer. Methods Engrg.*, 51:1009–1031, 2001.

[19] O.B. Tozoni and I.D. Maergoiz. *Rascet Trehmernih Elektromagnetnih Polei*. Tehnika, Kiev, 1974.

[20] J.R. Whiteman and L. Demkowicz (eds.). Proceedings of the Eleventh Conference on The Mathematics of Finite Elements and Applications. *Comput. Methods Appl. Mech. Engrg.*, 194(2-5), 2005.

[21] J. Yuan and A. Kost. A three-component boundary element algorithm for three-dimensional eddy current calculation. *IEEE Tran. on Mag.*, 30(5), September 1994.